Fall 12-16-2014

The Effect of pH and Counterion on the Size Distribution and Luminescence Lifetime of Terbium-Doped Lanthanum Nanocrystals

Sarah Baker

Honors Thesis Approval Page

Student Name: Sarah Baker

Title of Thesis: "The Effect of pH and Counterion on the Size Distribution and Luminescence Lifetime of Terbium-Doped Lanthanum Nanocrystals"

Accepted by the Honors Program and faculty of the Department of Chemistry and Biochemistry, University of San Diego, in partial fulfillment of the requirements for the Degree of Bachelor of Arts.

FACULTY APPROVAL

James P. Bolender	_____	_____
Faculty Project Advisor	Signature	Date
James Gump	_____	_____
Honors Program Director	Signature	Date

The Effect of pH and Counterion on the Size Distribution and Luminescence Lifetime of Terbium-Doped Lanthanum Nanocrystals

A Thesis

Presented to

The Faculty and the Honors Program

Of the University of San Diego

By

Sarah Kathleen Baker

Chemistry and Biochemistry

2014

Introduction

In recent years, nanoparticles have been applied to and have gained prevalence in fields such as chemistry, biology, the medical sciences, and biotechnology,[1] and have attracted the attention of medical researchers as potential microscopic drug delivery systems in the human body.[2] In particular, nanoparticles made with the lanthanides have shown themselves to be useful to many biological applications due to their unique luminescent properties.[1]

Because nanomaterials may be engineered to be between 1 and 100 nm in size, they are being explored for use in biological applications within the human body. In order for materials to be of use in the body, they must be small enough to leave through the kidneys,[2] and therefore 6 nm or smaller-sized particles are ideal.[3] These small particles have large surface area to volume ratios, and can therefore carry relatively large amounts of other materials, such as small molecules with pharmacological effects, on their surface.[2] This opens up the possibility for use in cellular therapy, gene therapy, immunizations, and detoxification,[4] and these small particles may be used for the delivery of drugs to the body.[2,4-6] These particles may also function in the field of oncology to aid in both visualizing and destroying cancerous tumors.[2,7]

Nanomaterials may be constructed of many different elemental compositions. Of particular interest are lanthanide nanoparticles, as the lanthanides have shown themselves to be useful in nanotechnology in a variety of ways. Applications include the detection of DNA concentration as low as 2 μg/mL,[8] use in fluorescent resonant energy transfer (FRET) as a method to detect interactions between proteins,[8,9] and efficient single-protein detection that has higher specificity than the most common method used for such detection, enzyme-linked immunoabsorbent assay (ELISA).[8] In addition, lanthanide

nanoparticles have shown potential in anti-fraud techniques as optical barcodes or markers on banknotes and important documents,[10] and have been explored for uses in such items as lasers and luminescent displays.[11]

A promising use for lanthanide nanoparticles is in imaging techniques. Lanthanide nanoparticles not only have promising optical properties, but also exhibit low cytotoxicity to cells which is crucial if they are to be biologically relevant.[2,4] Current imaging techniques face limitations due to the optical properties of the probes that are used which may not be ideal for distinguishing signal,[8] and because assays based on luminescence are fundamental to bioimaging techniques,[12] there is interest in creating probes that are more efficient and have higher sensitivity than probes already commonly in use. For example, green fluorescent protein (GFP) is a stain commonly used to visualize biomaterials of interest. However, GFP is imperfect because it loses luminescence over time as a consequence of instrumental photobleaching.[2,8] The lanthanides, in contrast, are resistant to photobleaching and also have well-defined, narrow emission bands, such that they may easily be distinguished from other background fluorescence.[2,12]

Multiple lanthanide ions can be co-doped into nanoparticles at various relative concentrations. Lanthanide-doped nanoparticles, which have a specific amount of a lanthanide element bound in their crystal structure, have several unique properties. These include high photostability[1,8,12,13] and long lifetimes as a result of the forbidden transitions among f-electron configurations.[8] In addition, these particles possess large Stokes shifts,[14] meaning that there is a large separation between the wavelength of absorption of light and that of the emission of light, which allows for ease in detecting

emission signals. Additionally, the lanthanides possess luminescent properties, also a result of the forbidden transitions among the f-electron configuration of the lanthanide ion.[8,9,15] Europium ions ($Eu^{3+)}$, terbium ions (Tb^{3+}), and gadolinium ions (Gd^{3+}) are unique in that they luminesce in every chemical environment, independent of the solvent they are in as well as other ions they are bound to.[11,16] In addition, many lanthanide ions (Ln^{3+}) have at least two luminescent states[11] that can be utilized for analytical purposes.

Not only do the lanthanides have special optical properties, but they also have notable magnetic properties.[13,17] Many of the lanthanide ions have a relatively large number of unpaired electrons, with Gd^{3+} and Eu^{2+} having seven unpaired electrons, and this leads to a high magnetic moment, allowing for these magnetic properties to be utilized. Magnetic resonance imaging (MRI) contrast agents yield a brighter MRI signal so that there is greater contrast between a tissue of interest and all surrounding tissue.[4,7,18] Currently, chelated Gd^{3+} is the most commonly used MRI contrast agent because of its high magnetic moment.[4,18] Since MRI contrast agents rely on magnetic properties, the lanthanides are being further explored as efforts are made to create improved contrast agents with increased sensitivity.

All of the fifteen lanthanide elements form stable tripositive ions and may be substituted for one another in a crystal lattice with little change in the crystal structure.[11,14] For this reason, lanthanum salt crystals may be doped with other lanthanides, which may be used to quantify concentration of the nanoparticles when the doped ion has luminescent properties that may be measured. Tb^{3+} and Eu^{3+} are less sensitive to vibrational quenching of luminescence by other vibrating molecules than are other lanthanide ions,[14] and thus may be most useful for this application.

Nanoparticles have attracted the attention of scientists for use with medical applications due to their ability to serve as drug delivery systems in the human body. However, in order for these particles to be utilized for these purposes, many conditions must be met; for this reason it is important to have methods to alter the shape, size, optical properties, and various other properties of nanoparticles. These properties may be controlled during synthesis by changing ionic strength, solvent used, dopant amounts, temperature, and pH. In this study, lanthanum fluoride (LaF_3), lanthanum chloride ($LaCl_3$), and lanthanum phosphate ($LaPO_4$) nanocrystals were synthesized under varied pH synthesis conditions. A capping group, *o*-phosphorylethanolamine, was used during synthesis to bind to the crystals, causing them to stop growing and keeping them on the nanoscale. Figure 2 demonstrates our hypothesis of how the capping group binds to the lanthanides in the crystal structure to stop crystal growth.

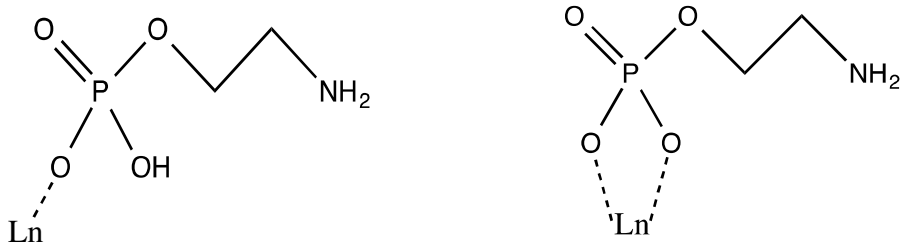

Figure 1. Possible binding of *o*-phosphorylethanolamine to lanthanide in crystal lattice.

It was hypothesized that nanocrystals synthesized in low pH conditions would be larger in size than those formed in higher pH solutions because the capping group, *o*-phosphorylethanolamine can be protonated at low pH values, preventing quick binding to the growing nanocrystals. It is crucial to determine optimum synthetic parameters so that nanoparticles are both small enough to pass through the kidneys and also have the ability to attach different functional groups so that they may be relevant to pharmaceutical

applications. The size distribution of terbium-doped lanthanide nanocrystals based upon varied counterions (fluoride, chloride, and phosphate) and pH conditions (pH 2-7) was quantified using the unique luminescent properties of terbium, and furthermore the quantum yield, or efficiency at emitting light, of these nanocrystals was explored using phosphorescence lifetime measurements.

Methods

Reagents

The lanthanide salts ($Tb(NO_3)_3 \cdot 6H_2O$ and $La(NO_3)_3 \cdot 6H_2O$) were purchased from Alfa Aesar and used without further purification. The capping group solution (*o*-phosphorylethanolamine) and the sodium salts (NaF, NaCl, and Na_3PO_4) were purchased from Sigma Aldrich and also used without further purification. The centrifuge tubes with membranes used for size separation were 3 K, 10 K, 50 K, 100 K, 300 K, and 1000 K Microsep™ Advance Centrifugal Devices purchased from the Pall Corporation.

Synthesis

Lanthanum fluoride (LaF_3), lanthanum chloride ($LaCl_3$), and lanthanum phosphate ($LaPO_4$) nanocrystals were synthesized as follows at a temperature of 37 °C with stirring. The syringe pump injected the lanthanide mixture (20% terbium (III) nitrate hexahydrate, 80% lanthanum (III) nitrate hexahydrate; 0.500 mL, 32.50 μmol, 65.0 mM) into a solution containing *o*-phosphorylethanolamine (3.25 mL, 260 μmol, 80.0 mM) and 0.125 M NaF (3.25 mL, 812 μmol, 0.250 M), 1.00 M NaCl (3.25 mL, 6.50 mmol, 2.00 M), or Na_3PO_4 (3.25 mL, 162 μmol, 0.050 M) at a flow rate of 500 uL per minute. The samples

were then incubated in a 37 °C shaker bath for 24 hours. The nanocrystal solutions were purified through centrifuge tubes with 3 K molecular weight cutoff membranes by centrifugation (4,000 rpm, 30 min, 4 X 10 mL H_2O washes) to eliminate any free floating particles in solution too small to be the desired nanocrystals. This entire synthesis procedure was completed for solutions of pH 2, 3, 4, 5, 6, and 7.

Size Separation

Nanocrystal solutions were centrifuged (4,000 rpm, 30 min, 3 X 10 mL H_2O washes) through membranes to separate out particles of specific molecular weight cutoff values (3 K – 10 K (0.3 – 1 nm), 10 K – 50 K (1 – 5 nm), 50 K – 100 K (5 – 10 nm), 100 K – 300 K (10 – 35 nm), 300 K – 1000 K (35 – 100 nm), and greater than 1000 K (> 100 nm) using Pall Microsep™ Advance Centrifugal Devices.

Luminescence Analysis

A PTI QuantaMaster-2 Spectrofluorometer was used to quantify luminescence. A reference scan of a Starna acrylic polymer reference cell with a polymethyl-methacrylate matrix was run in the spectrofluorometer with each set of data. This Starna acrylic polymer reference cell contains a stable reference material that allows luminescence scans from different days to be compared. Emission scans for each of the size-separated samples were run from 470 – 650 nm with an excitation of 350.5 nm. The luminescence values at 543 nm where a significant terbium peak was seen were used to compare concentrations relative to each other across size-separated samples based on luminescence intensity.

Lifetime Analysis

The phosphorescence lifetime of all nanocrystals at each pH, counterion, and size range was taken using a Jasco FP-6500 Spectrofluorometer. Forty scans were taken for each sample using a bandwidth of 10 nm. The excitation wavelength was set to 350.5 nm, while the emission wavelength was set to 540 nm. The lifetime was measured using Jasco Phosophorescence Lifetime Measurement software Version 1.07.02.

Results and Discussion

Quantification of Proportions of Each Size Fraction of Terbium-Doped Lanthanum Nanocrystals Based on Counterion and pH

This study aimed to look at the effect of both counterion used and pH of synthesis to see how this affected the size distribution of terbium-doped lanthanum nanocrystals. It was hypothesized that nanocrystals synthesized in low pH conditions would be larger in size than those formed in higher pH conditions, because the capping group, *o*-phosphorylethanolamine, can be protonated at low pH values, preventing quick binding to the growing nanocrystals (Figure 1). Subsequently, the luminescence lifetimes of the nanocrystals were examined to give insight into effects of counterion, pH, and nanocrystals size on the quantum yield of these nanocrystals.

Terbium-doped lanthanum nanocrystal synthesis efficiency was dependent on both counterion and pH of synthesis (Figure 2), as shown by fluorescence emission scan intensities that were run for all samples prior to size separation.

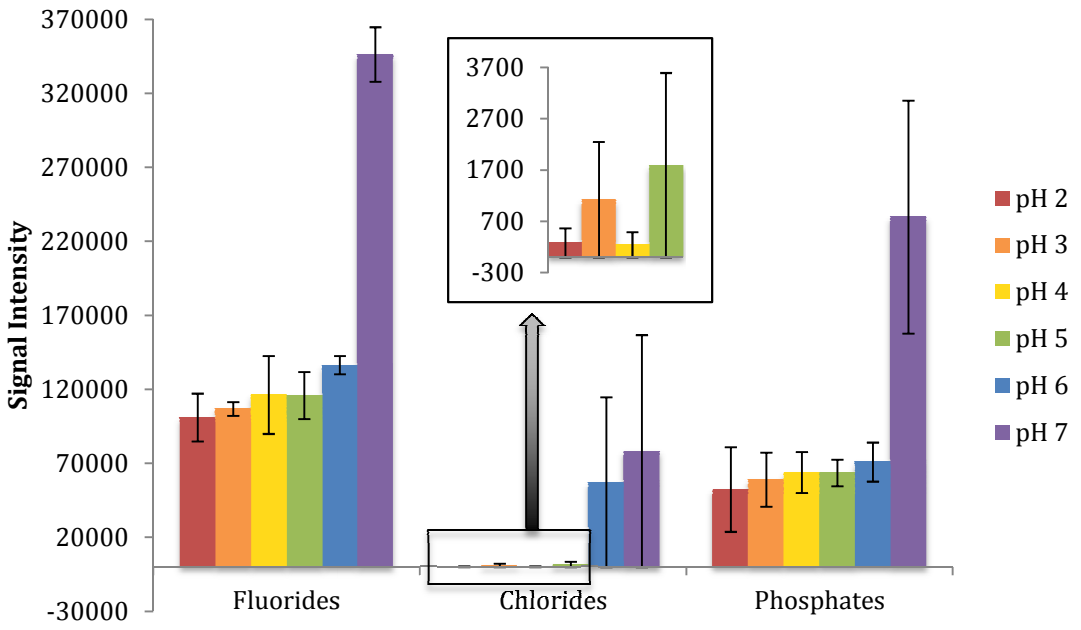

Figure 2. Emission signal intensities for LaF_3, $LaCl_3$, and $LaPO_4$ nanocrystals prior to size separation at pH 2, 3, 4, 5, 6, and 7 at 543 nm quantified on PTI QuantaMaster-2 Spectrofluorometer with excitation at 350.5 nm.

In this study, it was assumed that signal intensities are indicative of relative amounts of each nanocrystal in solution. For both LaF_3 and $LaPO_4$ nanocrystals, the best synthesis yield was found for pH 7 nanocrystals, which had a more than 3-fold increase in yield over all other nanocrystals synthesized at lower pH values for each counterion. The $LaCl_3$ nanocrystals had a significantly lower synthesis yield overall, especially for pH 2, 3, 4, and 5 nanocrystals. All three counterions had increasing yield with increasing pH except $LaCl_3$ nanocrystals at pH 3 and 4. It is possible that signal intensity was too low for the $LaCl_3$ nanocrystals, resulting in this break in the trend because more error in measurements was likely. Overall, it appears that pH 7 synthesis conditions result in optimum yield, with phosphate and fluoride nanocrystals being formed in the greatest amounts.

Following size separation, fluorescence emission scan intensities were taken for each size fraction. Figure 3a-c shows how the percentages of size fractions vary with pH for the lanthanide fluorides, chlorides, and phosphates, respectively.

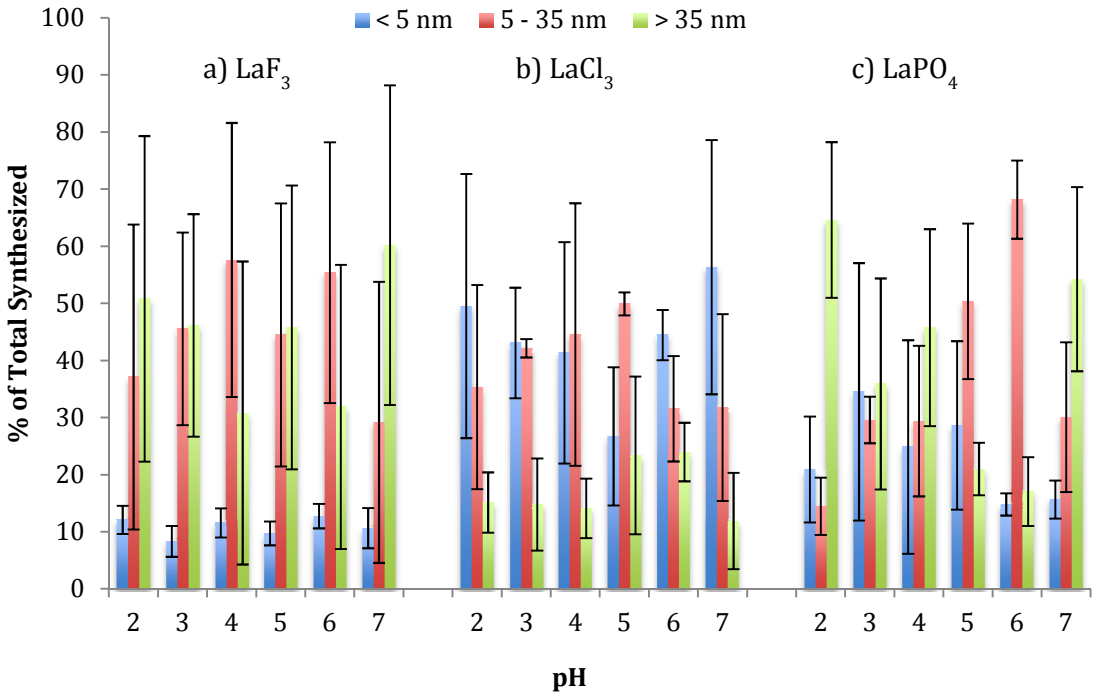

Figure 3. Graph showing the effect of pH on the percent of each size fraction synthesized for the 20% Tb LaF_3 (a), $LaCl_3$ (b), and $LaPO_4$ (c) nanocrystals using fluorescence emission intensity at 543 nm quantified on PTI QuantaMaster-2 Spectrofluorometer (excitation = 350.5 nm). Quantification of amounts of each size fraction was calculated assuming amount of nanocrystals created is proportional to luminescence.

Since amount of nanocrystals created was assumed to be proportional to luminescence, this provided a way to quantify the relative proportion of each size range created. The larger size fractions (5 – 35 nm and > 35 nm) tended to dominate the LaF_3 nanocrystals, regardless of the pH, while the smallest size fraction (< 5 nm) was consistently only about 10% of the sample synthesized (Figure 3a). This may be due to the insolubility of the lanthanide fluorides ($K_{sp} = 10^{-17.9}$)[19]. Because the lanthanide

fluorides are insoluble in water, the thermodynamic driving force will bring the fluoride and lanthanide ions together to make solid crystals. Hence, ions will readily attract one another to form crystals, and smaller crystals will be less likely to form since smaller crystals form from a fewer number of ions coming together. This issue may be combatted by using lower concentrations of reactants during synthesis in order to get smaller crystals forming throughout a more dilute solution.

An opposite trend was seen for the $LaCl_3$ nanocrystals (Figure 3b). The smaller size fractions tended to dominate the $LaCl_3$ nanocrystals and a low proportion of the largest size fraction (greater than 35 nm) was synthesized, independent of pH (Figure 3b). $LaCl_3$ is highly soluble (49.73 ± 0.02 wt % at 35 °C)[20] and will thermodynamically be more likely to exist as ions in solution at equilibrium;[21] therefore ions will not as readily attract one another to form a crystal structure, which could contribute to this result. In order to combat this solubility of the chlorides, a higher concentration of NaCl was used in the synthesis. However, the $LaCl_3$ nanocrystals still had very low synthesis yields (Figure 2).

While both the LaF_3 and $LaCl_3$ nanocrystals followed different trends than predicted by the hypothesis, that lower pH synthesis conditions would yield larger nanocrystals synthesized, the $LaPO_4$ nanocrystals showed a trend that is consistent with this hypothesis (Figure 3c). As the pH decreased from pH 6 to 2, the proportion of the largest size fraction (greater than 35 nm) of $LaPO_4$ nanocrystals increased, whereas the middle fraction (5 – 35 nm) decreased in proportion. Therefore, the $LaPO_4$ nanocrystals were generally increasing in size as a function of decreasing pH. This result follows what was predicted in the hypothesis, that low pH nanocrystals will be larger in size than those

formed in higher pH solutions. When protonated, the capping group, *o*-phosphorylethanolamine, will be less likely to bind to the lanthanide and stop crystal growth (Figure 1). In contrast, at more basic pH values, the phosphate on this capping group will likely be deprotonated, carrying a negative charge, which can bind to the lanthanide. Therefore, at low pH values, the crystals should be able to grow longer before the capping group stops them, yielding larger crystals. However, this trend was broken for pH 7 nanocrystals, which showed a large proportion of greater than 35 nm nanocrystals. This may be due to the fact that lanthanide phosphate has a pKa value at 7.21.[21] At about pH 7, 2 of the oxygens on the phosphate group will be deprotonated, allowing for quicker and more efficient binding to the lanthanide than at lower pH values. As predicted by Advanced Chemistry Development Software V11.0, the capping group does not have its second pKa value until 10.65,[22] so will be less efficient at binding to the lanthanide than the phosphate counterion is. This effect of the phosphate counterion competing with the weak-base equilibrium of the capping group could influence this increase in size at pH 7. To verify that this may be the reason for this effect, a future study will look at relative size distributions of these nanocrystals as the pH of synthesis is increased to between 8 and 11 pH units.

For the $LaCl_3$ nanocrystals, the only weak acid-base equilibrium is that of the capping group. However, both fluoride and phosphate ions act as weak bases in solution.[21] For this reason, when there are protons in solution, fluoride and phosphate ions may become protonated. When these anions are protonated, they will be unable to bind to the lanthanum or terbium cation, making lanthanide nanocrystals. We have to

account for the acid-base behavior of both the capping group and the counterion of the salt when explaining the size trends seen at various pH values.

It should be noted that error was significant between replicates of synthesized nanocrystals at particular pH values. Because there was significant variability in the data, this gives evidence that there are inconsistencies in the method of nanocrystal synthesis and/or size separation. A more consistent method should be determined to try to reduce this variability between replicates so that data will have more validity. In addition, statistical tests must be conducted before any true differences between relative proportions of nanocrystals of different sizes may be claimed.

Fluorescent Lifetime Measurements of Each Size Fraction of Terbium-Doped Lanthanum Nanocrystals Based on Counterion and pH

Figures 4, 5, and 6 show how the fluorescence lifetime varies with pH for each size fraction synthesized for the lanthanide fluorides, chlorides, and phosphates, respectively.

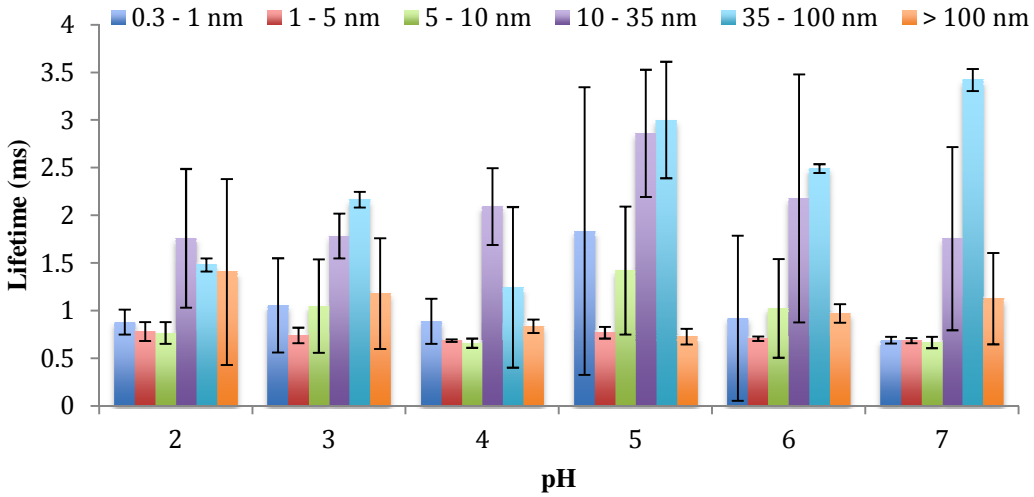

Figure 4. Effect of pH on fluorescence lifetime of size fractions of LaF_3 nanocrystals as determined by a Jasco FP-6500 Spectrofluorometer with excitation wavelength at 350.5 nm and emission wavelength at 540 nm.

It was found that the lifetime of LaF_3 nanocrystals exhibited a size-dependence (Figure 4). These nanocrystals showed increased lifetime values for the 35 – 100 nm fractions, as well as the 10 – 35 nm fractions. Curiously, the smallest fractions, 0.3 – 1 nm, had small lifetime values, but so did the largest size fraction, greater than 100 nm. Therefore it cannot be concluded that the lifetime is directly affected by the size of particles, but there must be some other factor also playing a role. It does not appear that there is a pH dependence on lifetime measurement for these nanocrystals.

The $LaCl_3$ nanocrystals showed a drastically different result, and lifetimes were relatively consistent across both size and pH (Figure 5).

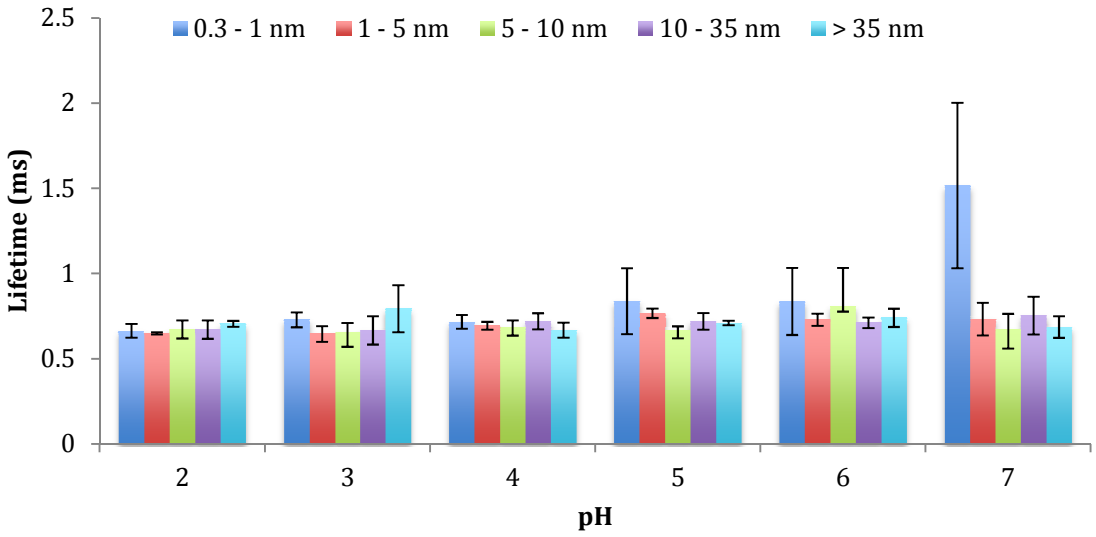

Figure 5. Effect of pH on lifetime of size fractions of $LaCl_3$ nanocrystals as determined by a Jasco FP-6500 Spectrofluorometer with excitation wavelength at 350.5 nm and emission wavelength at 540 nm.

The $LaCl_3$ nanocrystals showed no pH or size fraction dependence upon size. Across both of these factors, the lifetime stayed the same, about 0.7 ms (Figure 5), except for the

smallest size fraction (0.3 – 1 nm) at pH 7. This discrepancy may be due to the large amount of error in lifetime measurement of this fraction of nanocrystals. The $LaCl_3$ nanocrystals showed different behavior than both the LaF_3 (Figure 4) and $LaPO_4$ (Figure 6) nanocrystals, yielding consistent lifetime data that was most reproducible, as evident by the reduced error in these measurements when compared to the other two types of nanocrystals synthesized. While the reason for this is not yet known, the chlorides differ from both the fluorides or phosphates because they do not show the same acid-base equilibrium that the other two counterions do,[21] which could explain why the chlorides have more consistent luminescence lifetimes across pH and size.

The $LaPO_4$ nanocrystals did not have as consistent of lifetime measurements as did the $LaCl_3$ nanocrystals, and a clear pH or size dependence was not found either (Figure 6).

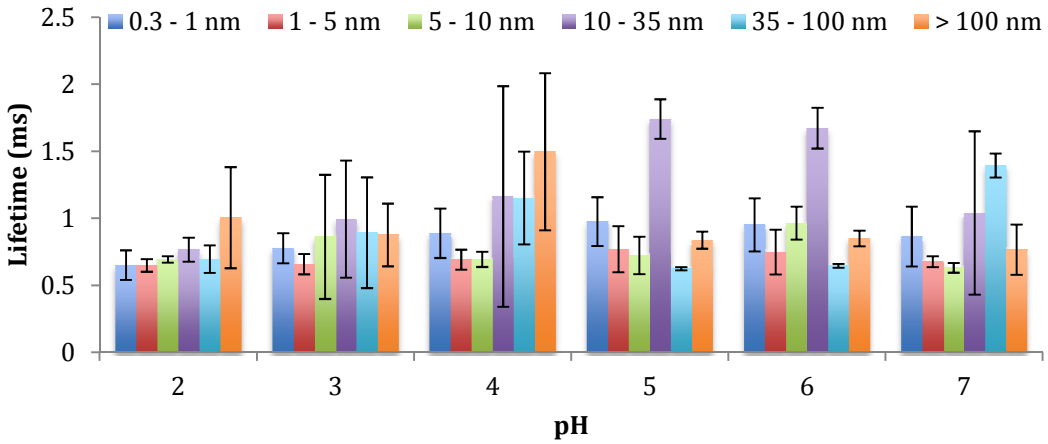

Figure 6. Effect of pH on lifetime of size fractions of $LaPO_4$ nanocrystals as determined by a Jasco FP-6500 Spectrofluorometer with excitation wavelength at 350.5 nm and emission wavelength at 540 nm.

The $LaPO_4$ nanocrystals did not show a clear trend in lifetime measurement based on pH or size fraction (Figure 6). However, the smallest size fractions (0.3 – 1 nm, 1 – 5 nm, and 5 – 10 nm) showed relatively consistent lifetime measurements across pH of synthesis. This trend is not evident for the three larger size fractions, with the 10 – 35 nm size fraction showing the most lifetime variability across pH. For instance, the 10 – 35 nm size fraction clearly has higher lifetime values at pH 5 and 6 than at pH 2. Data will be processed through Prism GraphPad statistical analysis software to determine if any lifetime measurements across pH or size fraction are significantly different; since some lifetime measurements did have a large amount of error, this makes conclusions about true lifetime differences indeterminate at this time.

Conclusions

We have shown that the size of terbium-doped lanthanum nanocrystals is affected by both the pH of synthesis and the counterion used in the crystal structure. In order to use lanthanide nanocrystals for biological applications, the size of these particles must be carefully controlled such that particles are less than 6 nm so that they may exit the body through the kidneys. Based on the results of the size distribution of terbium-doped lanthanum nanocrystals, synthesis of fluoride and chloride terbium-doped lanthanum nanocrystals cannot be controlled by altering pH; however, terbium-doped lanthanum phosphate nanocrystals showed a pH dependence, giving evidence that pH of synthesis may be used to control the synthesis size of these nanocrystals. Future work will involve altering the temperature of synthesis to see how this effects the size distribution. Finding

the correct synthesis conditions to synthesize nanocrystals that are exclusively less than 6 nm in size is an ultimate goal of this project.

A second goal of this project is to verify the assumption that the luminescence intensity measured on a spectrofluorometer is proportional to the amount of nanocrystals in solution. Measuring the lifetime of the lanthanide nanocrystals gives us insight into the quantum yield, or efficiency at emitting light, of these particles. Based on a quantum yield formula used by Du *et al.*, the lifetime of these nanocrystals should be directly proportional to their quantum yield.[23] A further direction of this research is to actually quantify the quantum yield of these nanoparticles. If there are differences in quantum yield that are dependent upon the pH or size of the nanocrystals, this must be implemented into the calculation of relative proportions of each size fraction of nanocrystal synthesized.

In addition, lifetime results have interesting applications for creating lanthanide nanocrystals that are to be used as optical probes or other luminescent materials, since the best materials for these applications will be those which have the highest quantum yield.

References

(1) Wang, G.; Peng, Q.; Li, Y., Lanthanide-Doped Nanocrystals: Synthesis, Optical-Magnetic Properties, and Applications. *Accounts of Chemical Research* **2011,** *44* (5).

(2) Kelkar, S. S.; Reineke, T. M., Theranostics: Combining Imaging and Therapy. *Bioconjugate Chemistry* **2011,** *22*, 1879-1903.

(3) Longmire, M. R.; Ogawa, M.; Choyke, P. L.; Kobayashi, H., Biologically Optimized Nanosized Molecules and Particles: More Than Just Size. *Bioconjugate Chemistry* **2011,** *22*, 993-1000.

(4) Mailander, V.; Landfester, K., Interaction of Nanoparticles with Cells. *Biomacromolucules* **2009,** *10*, 2379-2400.

(5) Manus, L. M.; Mastarone, D. J.; Waters, E. A.; Zhang, X.-Q.; Schultz-Simka, E. A.; MacRenaris, K. W.; Ho, D. H.; Meade, T. J., Gd(III)-Nanodiamond Conjugates for MRI Contrast Enhancement. *Nano Letters* **2010,** *10*, 484-489.

(6) Chen, S.; Wang, L.; Duce, S. L.; Brown, S.; Lee, S.; Melzer, A.; Cushieri, S. A.; Andre, P., Engineered Biocompatible Nanoparticles for *in Vivo* Imaging Applications. *Journal of the American Chemistry Society* **2010,** *132*, 15022-15029.
(7) Alric, C.; Taleb, J.; Le Duc, G.; Mandon, C.; Billotey, C.; Meur-Herland, A. L.; Brochard, T.; Vocanson, F.; Janier, M.; Perriat, P.; Roux, S.; Tillement, O., Gadolinium Chelate Coated Gold Nanoparticles As Contrast Agents for Both X-ray Computed Tomography and Magnetic Resonance Imaging. *Journal of the American Chemical Society* **2008,** *130*, 5908-5915.
(8) Bouzigues, C.; Gacoin, T.; Alexandrou, A., Biological Applications of Rare-Earth Based Nanoparticles. *ACS Nano* **2011,** *5* (11), 8488-8505.
(9) Charbonniere, L. J.; Hildebrandt, N.; Ziessel, R. F.; Lohmannsroben, H.-G., Lanthanides to Quantum Dots Resonance Energy Transfer in Time-Resolved Fluoro-Immunoassays and Luminescence Microscopy. *Journal of the American Chemical Society* **2006,** *128*, 12800-12809.
(10) Das, S.; Powe, A. M.; Baker, G. A.; Valle, B.; El-Zahab, B.; Sintim, H. O.; Lowry, M.; Fakayode, S. O.; McCarroll, M. E.; Patonay, G.; Li, M.; Strongin, R. M.; Geng, M. L.; Warner, I. M., Molecular Fluoresence, Phosphorescence, and Chemiluminescence Spectrometry. *Analytical Chemistry* **2011,** *84*, 597-625.
(11) Cross, A. M.; May, P. S.; van Veggel, F. C. J. M.; Berry, M. T., Dipicolinate Sensitization of Europium Luminescence in Dispersible 5%Eu:LaF_3 Nanoparticles. *Journal of Physical Chemistry* **2010,** *114*, 14740-14747.
(12) Chengelis, D.; Yingling, A. M.; Badger, P. D.; Shade, C. M.; Petoud, S., Incorporating Lanthanide Cations with Cadmium Selenide Nanocrystals: A Strategy to Sensitize and Protect Tb(III). *Journal of the American Chemical Society* **2005,** *127*, 16752-16753.
(13) Wang, L.; Yang, Z.; Zhang, Y.; Wang, L., Bifunctional Nanoparticles with Magnetization and Luminescence. *Journal of Physical Chemistry* **2009,** *113*, 3955-3959.
(14) Montgomery, C. P.; Murray, B. S.; New, E. J.; Pal, R.; Parker, D., Cell-Penetrating Metal Complex Optical Probes: Targeted and Responsive Systems Based on Lanthanide Luminescence. *Accounts of Chemical Research* **2008,** *42* (7), 925-937.
(15) Bovero, E.; van Veggel, F. C. J. M., Conformational Characterization of Eu^{3+}-Doped LaF_3 Core-Shell Nanoparticles through Luminescence Anisotropy Studies. *Journal of Physical Chemistry* **2007,** *111*, 4529-4534.
(16) Mahalingam, V.; Mangiarini, F.; Vetrone, F.; Venkatramu, V.; Bettinelli, M.; Speghini, A.; Capobianco, J. A., Bright White Upconversion Emission from $Tm^{3+}/Yb^{3+}/Er^{3+}$-Doped $Lu_3Ga_5O_{12}$ Nanocrystals. *Journal of Physical Chemistry Letters* **2008,** *112*, 17745-17749.
(17) Li, Z.; Zhang, Y.; Shuter, B.; Idris, N. M., Hybrid Lanthanide Nanoparticles with Paramagnetic Shell Coated on Upconversion Fluorescent Nanocrystals. *Langmuir Letters* **2009,** *25* (20), 12015-12018.
(18) Su, C.-H.; Sheu, H.-S.; Lin, C.-Y.; Huang, C.-C.; Lo, Y.-W.; Pu, Y.-C.; Weng, J.-C.; Shieh, D.-B.; Chen, J.-H.; Yeh, C.-S., Nanoshell Magnetic Resonance Imaging Contrast Agents. *Journal of the American Chemical Society* **2007,** *129*, 2139-2146.
(19) Durst, Richard A. *Ion Selective Electrodes*. U.S. Government Printing Office: Washington, D.C., 1969.

(20) Chen, Yang-Guo; Fang, Zheng; Yuan, Kun-Yang; Zhang, Quan-Ru; Wang, Shao-Fen. Solubilities of $LaCl_3$ in HCl Aqueous Solution at (25, 35, and 45) °C. *Journal of Chemical and Engineering Data* **2008**, *53* (1), 262-264.
(21) McMurry, John E.; Fay, Robert C. *General Chemistry: Atoms First*. Prentice Hall, New York, 2010.
(22) Advanced Chemistry Development Software V11.0.
(23) Du, Ya-Ping; Zhang, Ya-Wen; Yan, Zheng-Guang; Sun, Ling-Dong; Yan, Chun-Hua. Highly Luminescent Self-Organized Sub-2-nm EuOF Nanowires. *Journal of the American Chemical Society* **2009,** *131* (45), 16364-16365.